The structural (un)safety of tunnels explained by analytical approach

Dr. ir. C.B.M. Blom
Delft University of Technology, Holland Railconsult

From soft soil tunnelling practice it has been observed that the segmental thickness of the tunnel lining has a constant ratio to the tunnel diameter. Nevertheless many engineering models are published in literature and used in practice, which describe the structural behaviour of the tunnel lining. These models are used to analyse the structural safety of the tunnels. In this paper a new analytical approach is described which clearly reveals the influence on structural behaviour of longitudinal joints and lateral interaction between adjoining rings of the lining. Furthermore it is explained that a common missing parameter in today's models is the influence of the construction of the tunnel, and especially the influence of grouting. In this paper the influence of the grouting is assessed. It turns out that the observed lining thickness can be dominated by the influence of grouting.

Key words: tunnel, analytical, structural, safety, soft soil, grout

1 Introduction

Quote [3]: 'Wenn die Tübbinge wüßten, wie sie berechnet worden sind, sie gingen nicht kaputt, sie lachten sich kaputt!' (free translation: 'if tunnels should know how they are calculated, they would not fail by collapse, but they would die from laughter').

The above quote is typical for today's engineering of tunnels in soft soils. If one observes the practice of tunnelling it is obvious that the segmental thickness is a constant ratio to the diameter of the tunnel (figure 1), no matter the calculations carried out. One could ask the question why still calculations are made, since the result is always a segmental thickness stringently related to the diameter of the tunnel. On the other hand it is questionable whether today's engineering models predict real structural behaviour in the way that optimisation is possible.

This paper describes the theoretical background of engineering models often used in practice, denoted as 'homogeneous single ring models in soil'. Extensions on these models have been made regarding the explicit influence of the longitudinal joints and the interaction between adjoining rings. One very important issue is dealt with: the influence of grouting during the construction of tunnels. The models are compared and conclusions are drawn on their different behaviour in relation to structural safety.

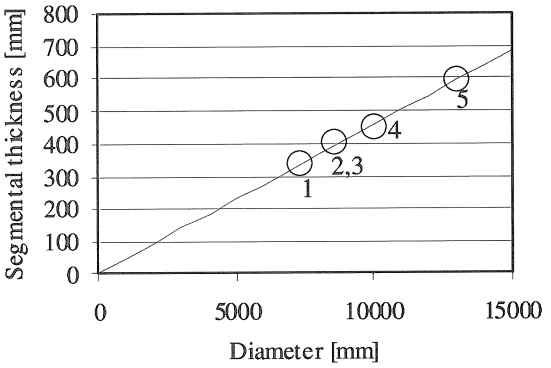

Nr	Project	Di [mm]	d [mm]	ratio d/Di
1	Second Heinenoord Tunnel	7600	350	1 / 21.7
2	Botlek Railway Tunnel	8650	400	1 / 21.6
3	Sophia Railway Tunnel	8650	400	1 / 21.6
4	Westerschelde Tunnel	10100	450	1 / 22.4
5	Green Heart Tunnel	13300	600	1 / 22.2

Figure 1. The segmental thickness as a function of the internal diameter of tunnels in the Netherlands.

2 Design models in literature

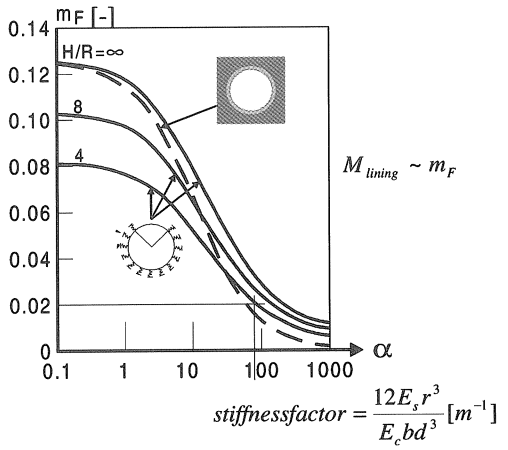

Figure 2. Design diagram for tunnels by Schulze-Duddeck [4].

In literature many design diagrams are found for tunnels surrounded by soils. A very familiar diagram is shown in figure 2. This diagram shows the tangential bending moments (on the vertical axis) as a function of a stiffness factor (on the horizontal axis). The stiffness factor includes the soil stiffness and the lining stiffness. The three different lines describe the relation for tunnels in several depths.

In a traditional structural design it feels comfortable when the structural thickness increases. The ultimate bearing capacity increases and in general the structural safety will increase. If a larger segmental thickness is applied for a tunnel, the stiffness factor on the horizontal axis of figure 2 decreases. As a consequence the internal tangential bending moment increases. An analysis shows that although the ultimate bearing capacity increases, still the safety factor decreases. It turns out that the development of the internal forces accelerates faster than the increase of the ultimate bearing capacity. Based on this relationship, one would choose a smaller lining thickness, since the safety factor would increase and the construction costs would decrease. Still the segmental thickness applied in practice has a steady ratio to the diameter of the lining.

The underlying theories for the design diagrams depend on basic assumptions, which have a tremendous influence on the model results. Some of the basic assumptions are:

- The longitudinal joints are excluded from the analysis. The ring is assumed to be a homogeneous ring (no longitudinal joints).
- There is no interaction between adjoining rings (no coupling forces).
- The tunnel is fully loaded and supported by soils (the influence of hardening grout during the construction is neglected).

In this paper it is illustrated what influence the above basic assumptions can have on the structural safety. It is notified that there are more basic assumptions which are not described here.

3 Principles of analytical models

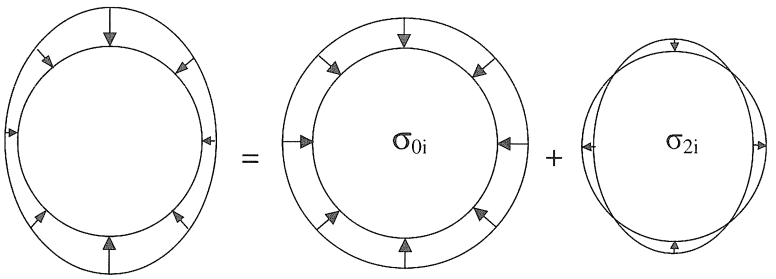

Figure 3. Idealised loading subdivided into a uniform load (σ_{0i}) and an ovalising load (σ_{2i}).

Figure 3 shows a loading definition that is often used in structural models for tunnels. It is arranged that there is equilibrium of forces. The loading is subdivided into a uniform and ovalisation loading. When a uniform pressure σ_{0i} loads the he tunnel, the tunnel uniformly deforms (called u_0, which means that the radius has a constant deformation around the tunnel circumference with a value u_0). The ovalisation loading σ_{2i} results in an ovalised tunnel deformation (called u_2, which means that de radius follows a sinus-shape deformation with a maximum amplitude with the value u_2). Floating of the tunnel (called u_1) is omitted.

The uniform compression of a single ring is given by:

$$u_0 = \frac{\sigma_o r^2}{E_c d}$$

where:

r = radius
E_c = Young's modulus of the concrete
d = segmental thickness
σ_0 = uniform load exerted on the lining

Considering the soil, the initial uniform loading σ_{0i} will be reduced to σ_0 by the elastic reaction of the soil, when the tunnel deforms. It is assumed that the elastic reaction of soil $\Delta\sigma_s$ is calculated by a very simple relation. In fact other relations can be used, but to illustrate the principle the following relation is used:

$$\Delta\sigma_s = \frac{E_s u_0}{r}$$

where:

E_s = elasticity of the soil

Both equations are rewritten with $\sigma_0=\sigma_{0i}-\Delta\sigma_s$ to:

$$u_0 = \frac{\sigma_{0i} r^2}{E_c d}(1-\alpha_0)$$

with

$$\alpha_0 = \frac{1}{\frac{E_c d}{E_s r}+1}$$

where α_0 is defined as the correction factor for the initial soil load, taking into account the unloading of the soil around the lining due to the elastic deformation of the lining. The factor α_j represents the part of the initial soil load, which disappears by the deformation of the lining and the elastic reaction of the soil. The remainder represents the load really exerted on the lining:

$\sigma_j = \sigma_{ji}(1-\alpha_j)$ [j=0 or j=2]

The ovalisation of the ring due to deformation of the segments only (by bending, excluding the influence of the longitudinal joints) is calculated by:

$$u_{2EI}(\varphi) = \frac{1}{9}\frac{\sigma_2 r^4 b}{E_c I}\cos(2\varphi)$$

where

$u_{2EI}(\varphi)$ = deformation by bending, as a function of φ
φ = angle, zero at the top
b = segmental width
I = moment of inertia of the segments

In the same way as for α_0 the factor α_2 is introduced for the loading part that is reduced by soil relaxation:

$$\alpha_2 = \frac{1}{\frac{3E_c d^3}{4E_s r^3} + 1}$$

Calculating u_{2EI} for a ring embedded in soil, means simply calculating α_2, reducing the initial soil load σ_{2i} with the reduction factor α_2 and calculating the structural behaviour of the ring (deformations, internal forces). It has turned out that α_0 is of minor influence. Therefore α_0 is mostly taken zero. The above theory can simply be applied to generate design diagrams as shown in figure 2.

4 Influence of longitudinal joints

In the theories quoted previously, the influence of the longitudinal joints is neglected. In [1] it is described how the influence of the longitudinal joints can be implemented. It is shortly explained here.

Assume a rotational stiffness c_r in the longitudinal joint (figure 4). The relation between the rotation θ_i in the longitudinal joint and the bending moment M_i in the longitudinal joint is calculated by:

$$\theta_i = \frac{M_i(\varphi)}{c_r}$$

Now an important basic assumption has to be made. To be able to estimate the rotation in the longitudinal joint, the bending moment in the joint has to be known. To calculate the bending moment the following equation is used:

$$M_\varphi = \frac{1}{3}\sigma_2 r^2 b \cos(2\varphi)$$

This relation actually is only valid for homogeneous rings without any discrepancies in bending stiffness. Without prove here, it is stated that a lining with equal sections (e.g. seven equal segments in a ring) and equal rotational stiffness in the longitudinal joints will have a bending moment directly following from this equation. The rotation θ_i of every longitudinal joint can be derived, if σ_2 is known.

Only considering the longitudinal joints, the deformation of the ring will appear only due to rotations occurring in the longitudinal joints. The question is now what influence a rotation has on the radial deformations (and consequently the reduction of the initial soil loading).

For example: what is the radial deformation between the top and bottom of the ring? Figure 4 shows half a ring with one longitudinal joint. Consider only the part of the ring between 0° and 180°. Suppose that the top of the ring is not rotating nor translating. The contribution of the rotation of the longitudinal joint at position i to the vertical displacement at the bottom of the ring is the rotation θ_i times the perpendicular distance to the vertical axis:

$$u_{v,bottom} = \theta_i \sin(\beta_i) r_s$$

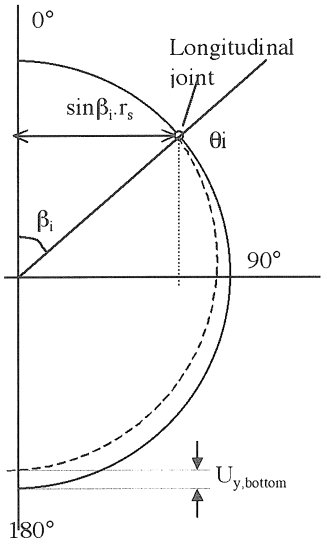

Figure 4. Contribution of joint rotation to deformation.

Naturally this is only the contribution of one longitudinal joint. The total radial deformation between the top and bottom caused by the longitudinal joints will be (as function of σ_2):

$$u_{2top,lj} = \frac{A}{2} \sum_{0<\beta_i<180} \cos(2\beta_i)\sin(\beta_i) \tag{1}$$

with:

$$A = \frac{\sigma_2 r^3 b}{3c_r} \tag{2}$$

In a very similar way the average horizontal radial displacement can be assessed (or even displacements on an axis with arbitrary angle).

From the implementation of the longitudinal joints in a ring it turns out that the longitudinal joints reduce the bending stiffness of the ring. Of course this was expected. The equations can easily be translated into a design diagram, as shown in figure 5. The reduction factor ξ has to be multiplied with the homogeneous bending stiffness to incorporate the influence of the longitudinal joints on the total bending stiffness. The reduction factor ξ on the vertical axis is a function of the longitudinal joint configuration expressed in the factor on the horizontal axis (involving the contact height in the longitudinal joint l_t, the radius and the segmental thickness). The various lines express the number of segments that is used in a ring.

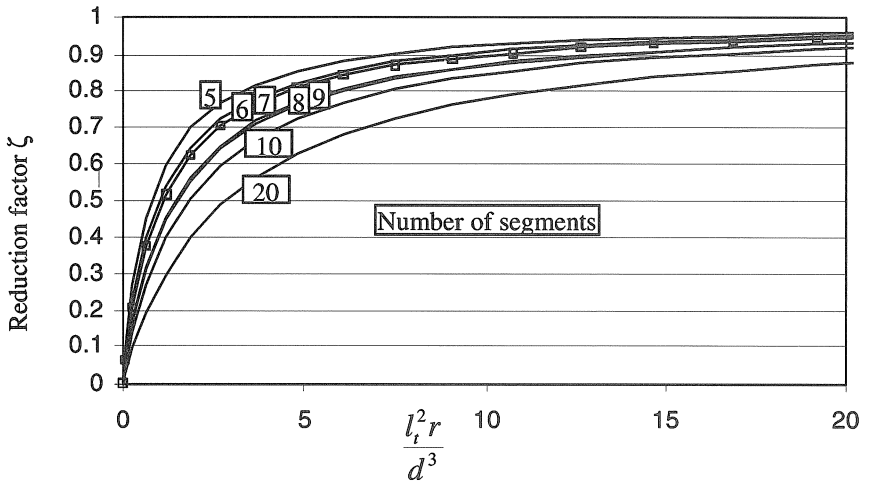

Figure 5. The reduction factor ξ for the bending stiffness as a function of the contact area in the longitudinal joint (l_t), the segmental thickness (d) and the radius, for several numbers of segments of a single ring.

5 Influence of lateral couplings

Adjoining rings are mostly assembled in a so-called masonry layout. This means that the longitudinal joints of the adjoining rings are not in line (the longitudinal joints of one ring are situated at the middle of the segments of the adjoining rings, see also figure 10). Figure 6 shows the first ring where the first longitudinal joint is positioned at 0° (at the top). The considered ring has seven segments and thus seven longitudinal joints. Figure 7 shows the second ring where the first longitudinal joint is positioned half a segmental arch length further. This means that the two adjoining rings have a masonry layout. It is obvious that the deformed shapes of the two rings are different, although they are both loaded by σ_2. Between the adjoining rings friction can occur. In this section it is assumed that the friction occurs concentrated near the positions of the longitudinal joints (where the largest deformation differences occur). In frame analyses the interaction is mostly modelled by use of radial springs.

It is assumed that the lateral joint springs are situated at every longitudinal joint (at i=0, 0.5, 1, .., 6.5). If the rings 1 and 2 are loaded by σ_2 without lateral joint interaction, due to rotations in the longitudinal joints the field of displacement in figure 6 and figure 7 occurs. Both the same deformations from rings 1 and 2 are presented together in figure 8.

The observation of these shapes reveals a double mirror symmetric deformation difference between the rings over both the horizontal and the vertical axis in figure 8. To predict the total deformation field, only 1 sector (e.g. 0 to 90°) has to be considered (figure 10). The next observation is that the lateral interaction forces are oriented in equal direction over the diameter (figure 9).

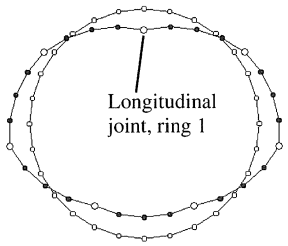

Figure 6. Shape ring 1.

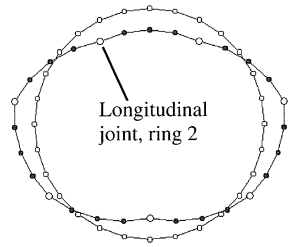

Figure 7. Shape ring 2.

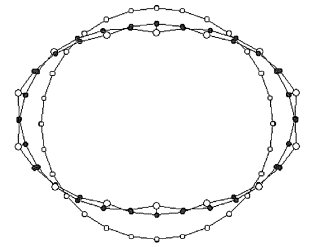

Figure 8. Shape ring 1 and 2 together.

For the bending moments in the segment near an interaction force P_i a relation has been derived (see [1 and 2]):

$$M_{pi} = \frac{1}{2} P_i r(1 - \frac{2}{\pi})$$

The interaction force P_i is the consequence of a differential displacement Δu_i of ring 1 and 2 at point *i*. Because the interaction is occurring as a result of a spring (in the model), P_i can be written as:

$P_i = k_v \Delta u_i$ and

$$M_{pi} = \frac{1}{2} k_v r(1 - \frac{2}{\pi}) \Delta u_i$$

where:

k_v = spring stiffness of the lateral radial coupling spring

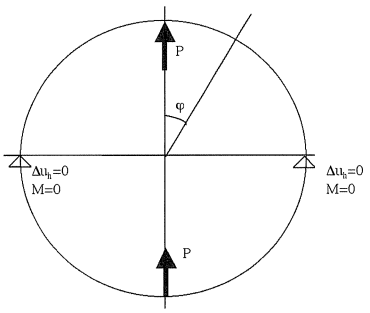

Figure 9. Equally directed lateral interaction forces at i=0 and 3.5.

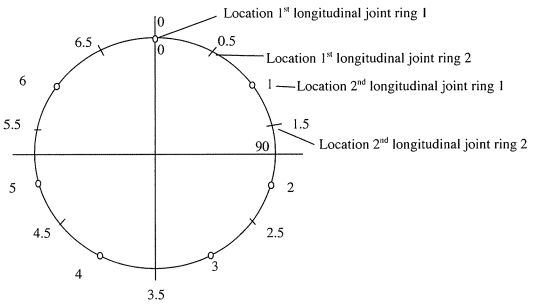

Figure 10. Considered section of rings with longitudinal joints.

In the theory it is assumed that P_i only influences the bending moments really close to point *i*. It has turned out that this assumption gives a very good approximation for the system behaviour (in comparison with both computer models and experimental references).

It is further assumed that the bending moment near *i* can be determined by superposition of $M_i(P_i)$ and $M_i(\sigma_2)$:

$$M_i = \frac{1}{3}\sigma_2 br^2 \cos(2\varphi_i) \pm \frac{1}{2}k_v r(1-\frac{2}{\pi})\Delta u_i$$

Here a cross relation applies. The tangential bending moments depend on Δu_i while Δu_i depends on the deformation from the rotation in the longitudinal joints due to the bending moments. Still this system of equations can be solved.

The rotation at a longitudinal joint is:

$$\theta_i = \frac{M_i}{c_{r,i}}$$

First the displacement of ring 1 at the top (φ=0°) is determined (only considering the ring section between 0° and 90°, figure 10) with the boundary condition that u_y at 90° is zero:

$$u_{0.1} = 0.5\theta_0 r + \theta_1 r(1-\sin\varphi_1) = 0.5r\theta_0 + 0.219r\theta_1$$

Next the displacement of ring 2 at the top (φ=0°) is calculated with the boundary condition that u_y at 90° is zero:

$$u_{0.2} = \theta_{0.5} r(1-\sin\varphi_{0.5}) + \theta_{1.5} r(1-\sin\varphi_{1.5}) = 0.56r\theta_{0.5} + 0.025r\theta_{1.5}$$

Now the differential displacement between the rings 1 and 2 is calculated:

$$\Delta u_0 = 0.5r\theta_0 - 0.56r\theta_{0.5} + 0.219r\theta_1 - 0.025r\theta_{1.5}$$

At all points i within 0° ≤ φ ≤ 90° the relation can be determined. Now a system of equations results that can be written as:

$$[S]\{\Delta u\} = \{f\}$$

or fully:

$$\begin{bmatrix} 0.09Br+1 & 0.1Br & 0.039Br & 0.0045Br \\ -0.9-0.039Br & 1 & 0 & 0 \\ -0.62-0.07Br & -0.078Br & 1 & 0 \\ -0.22-0.087Br & -0.14Br & -0.078Br & 1 \end{bmatrix} \cdot \begin{bmatrix} \Delta u_0 \\ \Delta u_{0.5} \\ \Delta u_1 \\ \Delta u_{1.5} \end{bmatrix} = \begin{bmatrix} 0.0387Ar \\ -0.0716Ar \\ -0.0376Ar \\ 0.0352Ar \end{bmatrix}$$

with:

$$A = \frac{\sigma_2 br^2}{c_r} \tag{6}$$

$$B = \frac{k_v r}{c_r} \tag{7}$$

To solve this system the stiffness matrix [S] has to be inverted, which is quite easily achieved with a spreadsheet. Now {Δu} is known:

$$\{\Delta u\} = [S]^{-1} \cdot \{f\}$$

From {Δu} the parameters P_i, M_i, θ_i, u_i can be solved.

To involve the soil support in the relations the displacement vector {Δu} should be written as a function of the loading σ_2. Then the interaction with the soil is taken into account by $\sigma_2=\sigma_{2i}-\Delta\sigma_s$. On the common, previously described, way again a factor α_2 follows, which represents the reduction of the initial loading by soil relaxation. The remaining part of the initial loading exerts on the lining

causing internal forces. Many examples how to obtain the solution for this problem are given in [1] and [2].

6 Influence of grouting

In the previous sections it was assumed that the tunnel is ideally embedded by the soil. The initial soil pressure is loading the ring, the ring is deforming and interacts with the soil. The soil reaction is schematised as a support bedding around the ring.

In practice the tunnel is assembled within the Tunnel Boring Machine (TBM). Since the TBM has a larger diameter than the tunnel itself, there is a gap between the tunnel and the soil. During the excavation this gap is injected with a liquid grout. It is expected that the grout is hardening in time. It is the question what pressures act on the tunnel during the liquid stage and how the grout supports the lining. These aspects are not incorporated in the traditional design models (the assembly stage is assumed to be not governing and therefore neglected). In this section some insight is given in the effect of the liquid state of the grout on the distribution of forces. The grout load on the lining is called 'the uplift loading case'.

It is assumed that the grout can develop an internal shear resistance. The shear resistance is limited to a plastic shear yield stress (viscoplasticity). This means that the grout has a resistance against flow, until the plastic shear yield stress limit is exceeded. From that point the grout is able to flow, but with the existence of a plastic shear yield stress (hardening or stiffening is neglected here).

The acting load in the uplift loading case on the lining is the sum of:
- The radial grout pressure, which is the sum of:
  - The water pressure.
  - The lining-grout contact pressure.
- The tangential grout loading (adhesion between the grout and the lining).
- The dead weight of the lining.

These loading components ensure the equilibrium of the vertical forces. The vertical component of the radial grout loading is equal to the dead weight (DW) of the tunnel and the vertical component of the tangential loading:

$$\int \sigma_{grout,radial,vertical} = DW + \int \tau_{grout,\tan,vertical}$$

The upward displacement of the tunnel starts when the increase of the grout pressure at the top (and decrease at the bottom) of the tunnel is insufficient to compensate the uplifting force of the grout. The plastic shear yield stress capacity limit of the grout can be exceeded. This is the moment that the grout starts to flow. A transportation process of the grout starts from the top of the lining in sideway direction. A large zone occurs where the plastic shear yield stress in the grout is exceeded if the upward movement of the tunnel is large enough. This means that along the circumference of a large part of the tunnel tangential stresses act, with the maximum value of the plastic shear

yield stress of the grout. Finally the equilibrium of the vertical forces is realised. This process of loading, the flow of the grout and the establishment of the equilibrium of vertical forces is analysed in a FEM calculation. The results of the FEM calculation are used to gain insight into the remaining grout pressure (water pressure and lining-grout contact pressure) and its distribution around the lining. In [1] a description is given how the pressure development by grouting around the tunnel can be determined with easy-to-use load models (for frame and FEM models). The load case that incorporates the grout is called the uplift loading case. It is shown in [1] how the grout load can be used in frame analyses.

The FEM analysis is based on linear elastic soil and lining behaviour. The lining is homogeneous and is assumed to have a Young's modulus of 70% (the influence of longitudinal joints) of plain concrete (36500Mpa). The grout is modelled using a viscoplastic material model, incorporating volume preservation and has an assumed plastic shear yield stress of $1.5*10^{-3}$ MPa. The tunnel is assumed to have an overburden of 12500mm and a diameter of about 14m. The level of the water table is at the surface ground level. In this FEM analysis it has been assumed that there is always contact between the lining and the grout (the lining-grout contact pressure never drops below zero). The initial grout stresses are due to the primary soil stresses.

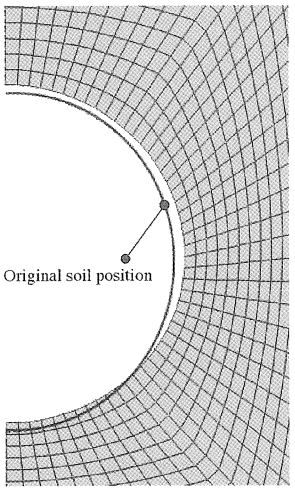

Figure 11. Soil movement due to the upward movement of the tunnel.

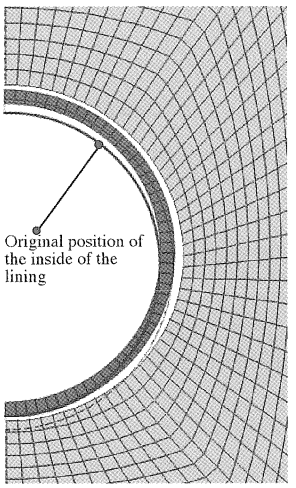

Figure 12. Movement and deformation of the lining due to the upward movement and pressure development.

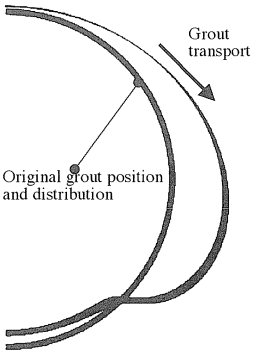

Figure 13. Flow and redistribution of the grout fluid (deformation scale 10:1).

Figure 11 shows the movement of the soil due to the uplift of the lining. Within the excavated and deformed soil the lining is moving and deforming (figure 12). The gap between the soil and the lining is filled with grout (figure 13). It is obvious that there is a grout transport between the top and the bottom of the ring. At the top of the ring the available space is smaller than at the bottom of the

ring. Due to the requirement of preserving grout volume, there is the flow of the grout. Because of the relative difference in deformation between the lining and the soil, there is a pressure development in the grout (figure 14). Figure 14 shows that the sum of the hydrostatic water pressure (C) and the grout-lining contact pressure (B) equals the grout pressure (A). The grout pressure (the water pressure and the lining-grout contact pressure) results in an uplift force that compensates the downward direct loading due to dead weight and tangential stresses at the grout-lining contact surface. It is obvious that the distribution of the grout pressure at the top of the lining shows a local increase of the grout pressure (figure 14). The grout pressure gradient (A) over the tunnel height is less compared to the gradient of the water pressure (C).

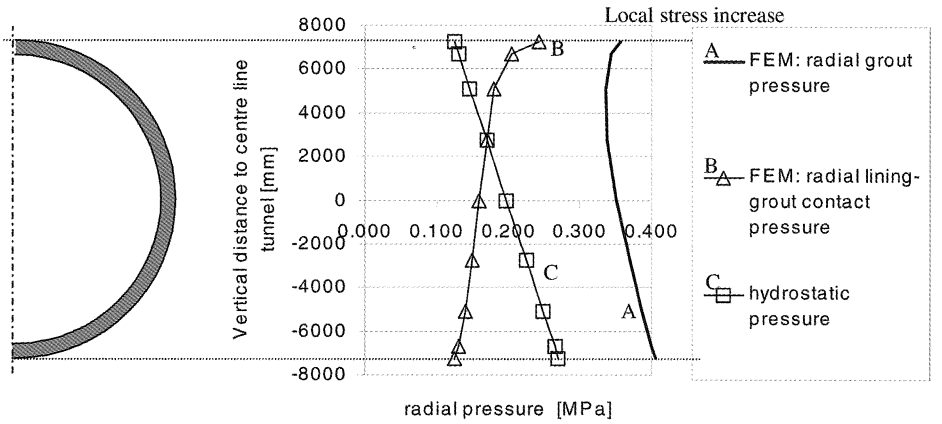

Figure 14. The radial pressure of the various loading components of the grout.

7 Interpretation of models in soils

Figure 15 shows a similar diagram as figure 2, but now also includes lines for models with explicit longitudinal joints and lateral couplings. The new lines can be compared to the 'basic' line from Schulze-Duddeck.

The model for the single homogeneous ring (section 3) is represented by line B. The solution agrees well with the basic line of Schulze-Duddeck (line A). Line C represents the single ring with the longitudinal joints. It is expected that the longitudinal joints reduce the bending stiffness of the tunnel. As a consequence the tunnel 'attracts' less forces. Therefore less bending moments are developed in the lining compared to the homogeneous rings. The influence of the double ring model with the lateral couplings is represented with line D. The ring interaction between the adjoining rings locally disturbs the bending moments. As a result the maximum tangential bending moments increase. That is why this line is higher than the previous lines.

In practice there is always discussion about the spring stiffness of the lateral coupling springs. Line E represents a lining system where the coupling stiffness k_v is infinite. As the figure shows, the

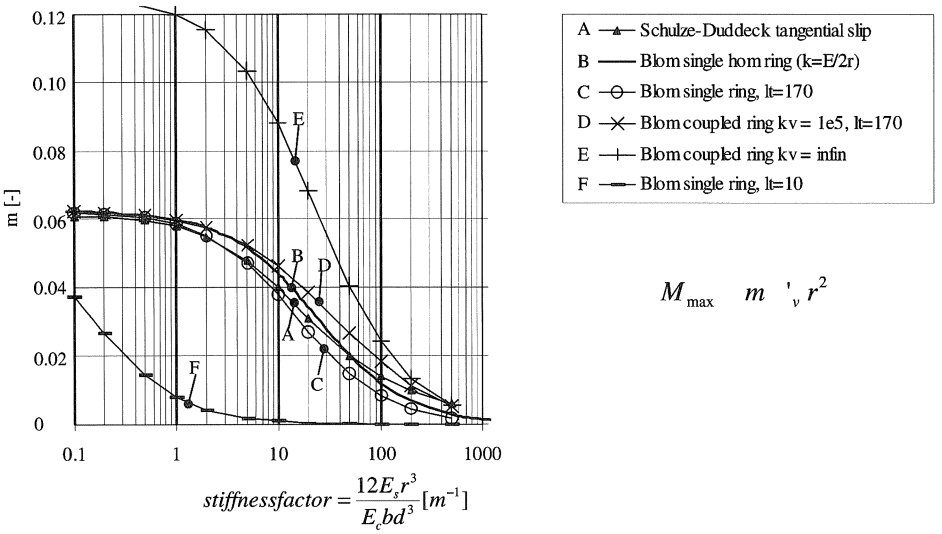

Figure 15. Comparison for the maximum tangential bending moments for the analytical solution and solutions from literature.

occurring maximum bending moments are much higher, but limited. On the other hand a lining can be assembled without ring interaction ($k_v = 0$) and longitudinal joints as hinges. This system is represented by line F. It is obvious that this system results in much lower tangential bending moments, because it's bending stiffness is very low. As a consequence, this system is highly depending on the soil support.

From figure 15 it becomes clear that bending stiffness of the lining plays a very dominant role. The stiffness ratio between the soil and the lining is one of the most important factors in these models. But still the issue remains that if the segmental thickness increases, the general structural safety factor might decrease. If one should design a tunnel only based on this diagram, the lining configuration should have low bending stiffness without ring interaction to increase the safety. In the following section it is illustrated what impact the construction stage (liquid grout in the uplift loading case) has on the structural safety, compared to design models with soil support.

8 Consequences of the grouting during construction in relation to structural safety

From the analysis of conventional load cases, it became clear that the bending stiffness of the lining has a reverse effect on the total safety of the system. The total stiffness of the lining increases when the lining thickness is increasing or longitudinal joints act stiffer. Besides, lateral couplings locally disturb the tangential bending moments. As a consequence the internal forces are increasing. The increase of the internal forces is larger than the increase of the ultimate bearing capacity of the segments due to the increase of the thickness. Consequently the load cases in the serviceability stage

(with soil support) show an increase of the safety with decreasing lining thickness.

Figure 16 shows the overall safety factors (M_u/M_{max}) for the lining of a tunnel in the two loading cases (the standard loading case for the models with soil support and the uplift loading case with liquid grout). On the horizontal axis the increasing lining thickness is given. On the vertical axis the safety factor to the ultimate capacity of the segments with reinforcement FeB500 Ø 10-100 is shown.

The standard load case shows a decrease of the safety factor when the segmental thickness increases as predicted in the former sections. If the lining becomes thicker than 600mm, the safety factor increases again. Then the lining is much stiffer compared to the soil and attracts all the forces without being supported by the soil. The soil support is especially useful to minimise extensive force development in the concrete lining. In the uplift loading case this support is omitted, because the grout is not hardened yet. The internal forces are much more constant when the segmental thickness increases, while the capacity of the segments increases. As a consequence the safety factor increases in the uplift loading case when the segmental thickness increases. The uplift loading case shows an increase of the safety factor when the lining thickness increases.

Based on the standard load case the segmental thickness should be chosen small. This means a minimum use of concrete, which reduces costs, and a maximum safety factor. Based on the uplift loading case the concrete thickness is chosen larger to have a minimum required safety factor. From the analyses [1] it has also become clear that during the assembly it has to be arranged that the grout pressure around the lining is sufficient and well distributed (too low or too high grout pressures cause lower safety factors [1]).

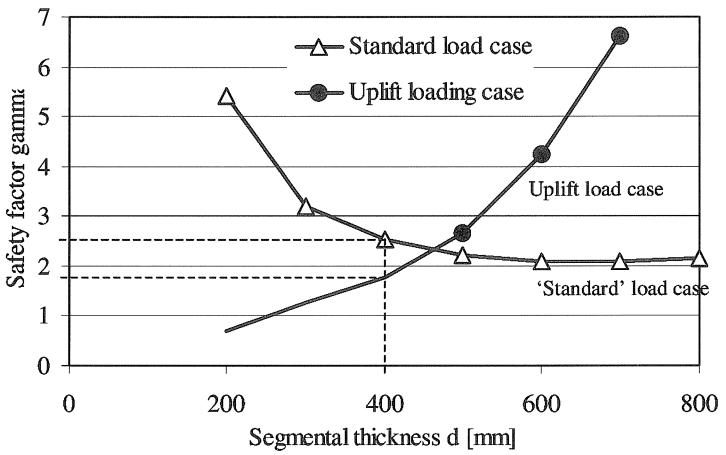

Figure 16. Safety factors for the standard and the uplift loading cases as a function of the segmental thickness.

9 Conclusions

It is concluded that the engineering models found in literature show an unexpected behaviour. Based on the models where the tunnel is fully supported by soil, the segmental thickness should be chosen smaller than the segmental thickness that is observed in today's practice. The applied segmental thickness in practice is based on the empirical rule that the segmental thickness is a steady ratio to the diameter of the tunnel. This empirical rule is now confirmed by the uplift loading case, where the tunnel is surrounded by liquid grout during the construction stage. In this load case the liquid grout plays a very dominant role.

It has turned out that the soil support has a major influence on the internal forces. When the soil support is omitted because of, for example, liquid grouting that is not hardened in a short time, the general safety of the lining can dangerously drop down. Or in other words: Once one can control the grouting process in a way that soil support is guaranteed, the segmental thickness can be optimised to be thinner. From the point of view of the serviceability stage (normal loading case) a thick lining is not necessary. When the segmental thickness is governed by, for example, the axial jack forces that are used during construction to forward move the TBM and exert enormous forces on the lining, for sure the segmental thickness is not optimal. Once the building process is controlled in a way that the serviceability stage is normative, then the more advanced models might be used to optimise the lining thickness. These models incorporate explicitly longitudinal joint rotations and lateral couplings between adjoining rings. It turned out the longitudinal joints and couplings are very important geometrical parts of the lining which can be used to optimise the structural behaviour of the lining.

It is concluded that the basic assumption made for models often used in practice that the construction stage is not a governing stage, is a major risk for the structural safety.

Acknowledgement

This paper is mainly based on the work done in the Ph.D. thesis, "Design philosophy of segmented linings for tunnels in soft soils" [1], which was funded by Holland Railconsult, The Ministry of Transports and Water Management and TNO Building and Construction Research. The thesis has been awarded with the international fib diploma 2003 for young researchers at 5 may 2003 in Athens, Greece.

References

[1] **Blom C.B.M.**, 2002, Ph.D. thesis, *"Design philosophy of segmented linings for tunnels in soft soils"*, ISBN 90-407-2366-4, DUP, Delft, The Netherlands.

[2] **Blom C.B.M.**, 2002, *"Background document for Lining behaviour - Analytical solutions of coupled rings in soil"*, Delft University of Technology 25.5-01-15.

[3] **Duddeck Heinz**, *'Ingenieure in ihrer Zeit, Laudationes Lebenswege'*, ISBN 3-926031-90-5, Braunsweig, Germany.

[4] **Duddeck Heinz**, *'Analysis of linings for shielddriven tunnels'*, Braunsweig, Germany.